Simple Matrix Method with Nonhomogeneous Space Increments in Finite Difference Method

Sungki Min[1], Hunhee Kim[1], Soo Won Chae[2], and *Junghwa Hong[1]

[1] Department of Control and Instrumentation Engineering, Korea University, Sejong, Republic of Korea.
[2] Department of Mechanical Engineering, Korea University, Seoul, Republic of Korea.

*Corresponding author: hongjh32@korea.ac.kr

Abstract

FDM (finite difference method) has advantages for direct code expansion to numerically solve PDE (partial differential equation). In contrast to finite element method configured with nonhomogeneous element size based on interested region, a constant increment size of element or grid is used in existing FDM. As a result, the calculation near boundary could be inaccurate and incomplete. Particularly, in electrokinetics, except for diffuse layer (about $10\sim10^4$ Angstrom) near solid and fluid interface, calculation of the charge density distribution with having the same and fine space increments at another region is inefficient and could meet the catastrophic memory lack error. In this study, we provide a method how to make the nonhomogeneous space incremental FD grid and to configure PDE having complicated and mixed boundary conditions (e.g. Dirichlet and Neumann) with suggested simple matrices. The suggested FDM using the nonhomogeneous increment of fine grids near the boundaries and interfaces could increase the accuracy of solutions and efficiency of calculations.

Keywords: Finite Difference Method, Partial Differential Equation, Nonhomogeneous Increment, Dirichlet and Neumann Boundary Conditions

Introduction

Solutions of electrokinetic problems are important to understand living bone remodeling processes by electromechanical transduction effects on osteocytes, osteoclasts and osteoblasts. Since this electromechanical transduction postulation about bone remodeling processes requires the existence of ionic interstitial bone fluid flow in bone tissues, the resulting streaming potential is being focused on bone mechanics as a remodeling stimulation on bone cells [Pienkowski and Pollack (1983); Zhang et al. (1997)]. The streaming potential is about coupled phenomenon described by elasticity of bone tissue, fluid mechanics of interstitial fluid flow through canaliculi and lacunae, and electricity of charged ions in bone fluid.

In addition, the streaming potential that is an electrokinetic phenomenon is closely related to electrical charge on the wall of lacunocanalicular flow path. The streaming potential is very sensitively affected by the interface surface electrical potential of the canalicular wall [Ahn and Grodzinsky (2009)]. Since bone is a piezoelectric material [Bassett (1968)], the surface electrical potential of the canalicular wall is changed by the elasticity of bone tissue. As a result, a full analysis including transient behavior of streaming potential can be achieved for the multi-physical study of bone tissue after firstly considering effects of its piezoelectricity on the just boundaries of the lacunocanalicular flow paths on the transient electrokinetics.

To solve electrokinetic problems using FDM, except for diffuse layer (about $10\sim10^4$ Angstrom) near solid and fluid interface, calculation of charge density distribution with having the same space increments at another region is inefficient. In this study, we provide a method how to make the nonhomogeneous space incremental FD grid and to configure PDE having complicated and mixed boundary conditions with suggested simple matrices. The suggested method is verified using the existing closed solution in the electrokinetics [ref].

Numerical Method

Notation and Definition

For the formulation used in this study, we used the following notations and definitions.

$$f_{i,j,k}^{\tau} \tag{1}$$

where subscript i, j, and k are the space incremental numbers; and superscript τ is the time incremental number. $i=1\sim L+1$; $j=1\sim M+1$; $k=1\sim N+1$; and $\tau=1\sim T+1$ where *i, j,* and *k* are the positive integer. f is a unknown quantity.

Position

The position is described as x_i, y_j, and z_k in the Cartesian coordinate, r_i, θ_j, and z_k in the cylindrical coordinate, r_i, θ_j, and ϕ_k in the spherical coordinates.

Variable Increment

The increment of the position or time is described by forward, backward and central difference.

$$\begin{aligned}(\Delta p)^{+} &= p^{+} - p^{0}\\ (\Delta p)^{-} &= p^{0} - p^{-}\\ (\Delta p)^{0} &= 0.5\left(p^{+} - p^{-}\right)\end{aligned} \tag{2}$$

where p means an arbitrary position, time, or value; superscripts $+$, $-$, and 0 mean forward, backward, and central infinitesimal approaches, respectively. In the Cartesian coordinate, time and spatial increments are represented by (3).

$$\begin{aligned}
&(\Delta t^{\tau})^{+} = t^{\tau+1} - t^{\tau} && (\Delta t^{\tau})^{-} = t^{\tau} - t^{\tau-1} && (\Delta t^{\tau})^{0} = 0.5\left(t^{\tau+1} - t^{\tau-1}\right)\\
&(\Delta x_i)^{+} = x_{i+1} - x_i && (\Delta x_i)^{-} = x_i - x_{i-1} && (\Delta x_i)^{0} = 0.5\left(x_{i+1} - x_{i-1}\right)\\
&(\Delta y_j)^{+} = y_{j+1} - y_j && (\Delta y_j)^{-} = y_j - y_{j-1} && (\Delta y_j)^{0} = 0.5\left(y_{j+1} - y_{j-1}\right)\\
&(\Delta z_k)^{+} = z_{k+1} - z_k && (\Delta z_k)^{-} = z_k - z_{k-1} && (\Delta z_k)^{0} = 0.5\left(z_{k+1} - z_{k-1}\right)
\end{aligned} \tag{3}$$

First Order Derivatives

The first order derivatives of time and space are described by (4).

$$\begin{aligned}
&\left(\frac{\Delta f}{\Delta t}\right)^{+} = \frac{f_{i,j,k}^{\tau+1} - f_{i,j,k}^{\tau}}{t^{\tau+1} - t^{\tau}} && \left(\frac{\Delta f}{\Delta t}\right)^{-} = \frac{f_{i,j,k}^{\tau} - f_{i,j,k}^{\tau-1}}{t^{\tau} - t^{\tau-1}} && \left(\frac{\Delta f}{\Delta t}\right)^{0} = \frac{f_{i,j,k}^{\tau+1} - f_{i,j,k}^{\tau-1}}{t^{\tau+1} - t^{\tau-1}}\\
&\left(\frac{\Delta f}{\Delta x}\right)^{+} = \frac{f_{i+1,j,k}^{\tau} - f_{i,j,k}^{\tau}}{x_{i+1} - x_i} && \left(\frac{\Delta f}{\Delta x}\right)^{-} = \frac{f_{i,j,k}^{\tau} - f_{i-1,j,k}^{\tau}}{x_i - x_{i-1}} && \left(\frac{\Delta f}{\Delta x}\right)^{0} = \frac{f_{i+1,j,k}^{\tau} - f_{i-1,j,k}^{\tau}}{x_{i+1} - x_{i-1}}\\
&\left(\frac{\Delta f}{\Delta y}\right)^{+} = \frac{f_{i,j+1,k}^{\tau} - f_{i,j,k}^{\tau}}{y_{j+1} - y_j} && \left(\frac{\Delta f}{\Delta y}\right)^{-} = \frac{f_{i,j,k}^{\tau} - f_{i,j-1,k}^{\tau}}{y_j - y_{j-1}} && \left(\frac{\Delta f}{\Delta y}\right)^{0} = \frac{f_{i,j+1,k}^{\tau} - f_{i,j-1,k}^{\tau}}{y_{j+1} - y_{j-1}}\\
&\left(\frac{\Delta f}{\Delta z}\right)^{+} = \frac{f_{i,j,k+1}^{\tau} - f_{i,j,k}^{\tau}}{z_{k+1} - z_k} && \left(\frac{\Delta f}{\Delta z}\right)^{-} = \frac{f_{i,j,k}^{\tau} - f_{i,j,k-1}^{\tau}}{z_k - z_{k-1}} && \left(\frac{\Delta f}{\Delta z}\right)^{0} = \frac{f_{i,j,k+1}^{\tau} - f_{i,j,k-1}^{\tau}}{z_{k+1} - z_{k-1}}
\end{aligned} \tag{4}$$

Second order derivatives

The second order derivatives are described by (5).

$$\frac{\partial^2 f}{\partial p^2}=\frac{\left(\frac{\Delta f}{\Delta p}\right)^{+}-\left(\frac{\Delta f}{\Delta p}\right)^{-}}{(\Delta p)^0}=\frac{\left(\frac{f^{+}-f^{0}}{p^{+}-p^{0}}\right)-\left(\frac{f^{0}-f^{-}}{p^{0}-p^{-}}\right)}{(\Delta p)^0}=\frac{f^{-}}{(\Delta p)^0(\Delta p)^-}-\frac{2f^{0}}{(\Delta p)^+(\Delta p)^-}+\frac{f^{+}}{(\Delta p)^+(\Delta p)^0} \quad (5)$$

Thus, the second order derivatives of time and space are described by (6).

$$\begin{aligned}
\frac{\partial^2 f}{\partial t^2}&=\frac{f^{\tau-1}_{i,j,k}}{(\Delta t^\tau)^0(\Delta t^\tau)^-}-\frac{2f^{\tau}_{i,j,k}}{(\Delta t^\tau)^+(\Delta t^\tau)^-}+\frac{f^{\tau+1}_{i,j,k}}{(\Delta t^\tau)^+(\Delta t^\tau)^0}\\
\frac{\partial^2 f}{\partial x^2}&=\frac{f^{\tau}_{i-1,j,k}}{(\Delta x_i)^0(\Delta x_i)^-}-\frac{2f^{\tau}_{i,j,k}}{(\Delta x_i)^+(\Delta x_i)^-}+\frac{f^{\tau}_{i+1,j,k}}{(\Delta x_i)^+(\Delta x_i)^0}\\
\frac{\partial^2 f}{\partial y^2}&=\frac{f^{\tau}_{i,j-1,k}}{(\Delta y_j)^0(\Delta y_j)^-}-\frac{2f^{\tau}_{i,j,k}}{(\Delta y_j)^+(\Delta y_j)^-}+\frac{f^{\tau}_{i,j+1,k}}{(\Delta y_j)^+(\Delta y_j)^0}\\
\frac{\partial^2 f}{\partial z^2}&=\frac{f^{\tau}_{i,j,k-1}}{(\Delta z_k)^0(\Delta z_k)^-}-\frac{2f^{\tau}_{i,j,k}}{(\Delta z_k)^+(\Delta z_k)^-}+\frac{f^{\tau}_{i,j,k+1}}{(\Delta z_k)^+(\Delta z_k)^0}
\end{aligned} \quad (6)$$

Laplacian

In the Cartesian coordinate, Laplacian of a quantity is described by (7).

$$\begin{aligned}
\nabla^2 f=&\frac{f^{\tau}_{i-1,j,k}}{(\Delta x_i)^0(\Delta x_i)^-}+\frac{f^{\tau}_{i+1,j,k}}{(\Delta x_i)^+(\Delta x_i)^0}+\frac{f^{\tau}_{i,j-1,k}}{(\Delta y_j)^0(\Delta y_j)^-}+\frac{f^{\tau}_{i,j+1,k}}{(\Delta y_j)^+(\Delta y_j)^0}+\frac{f^{\tau}_{i,j,k-1}}{(\Delta z_k)^0(\Delta z_k)^-}+\frac{f^{\tau}_{i,j,k+1}}{(\Delta z_k)^+(\Delta z_k)^0}\\
&-2\left(\frac{1}{(\Delta x_i)^+(\Delta x_i)^-}+\frac{1}{(\Delta y_j)^+(\Delta y_j)^-}+\frac{1}{(\Delta z_k)^+(\Delta z_k)^-}\right)f^{\tau}_{i,j,k}
\end{aligned} \quad (7)$$

Boundary Conditions

The Boundary conditions are defined on the interface locating at 1, L + 1, M + 1, and N + 1. Dirichlet boundary condition ($\phi=0$ at interface) could be formed as (8).

$$\begin{aligned}
&\text{x coordinate : } f^{\tau}_{1,j,k}=0 \text{ or } f^{\tau}_{L+1,j,k}=0 \text{ or } f^{\tau}_{1,j,k}=f^{\tau}_{L+1,j,k}=0\\
&\text{y coordinate : } f^{\tau}_{i,1,k}=0 \text{ or } f^{\tau}_{i,M+1,k}=0 \text{ or } f^{\tau}_{i,1,k}=f^{\tau}_{i,M+1,k}=0\\
&\text{z coordinate : } f^{\tau}_{i,j,1}=0 \text{ or } f^{\tau}_{i,j,N+1}=0 \text{ or } f^{\tau}_{i,j,1}=f^{\tau}_{i,j,N+1}=0
\end{aligned} \quad (8)$$

Neumann boundary condition ($\Delta\phi/\Delta x=0$ at interface) could be formed as (9).

$$\begin{aligned}
&\text{x coordinate : } f^{\tau}_{1,j,k}=f^{\tau}_{2,j,k} \text{ or } f^{\tau}_{L+1,j,k}=f^{\tau}_{L,j,k} \text{ or } f^{\tau}_{1,j,k}=f^{\tau}_{2,j,k} \text{ and } f^{\tau}_{L+1,j,k}=f^{\tau}_{L,j,k}\\
&\text{y coordinate : } f^{\tau}_{i,1,k}=f^{\tau}_{i,2,k} \text{ or } f^{\tau}_{i,M+1,k}=f^{\tau}_{i,M,k} \text{ or } f^{\tau}_{i,1,k}=f^{\tau}_{i,2,k} \text{ and } f^{\tau}_{i,M+1,k}=f^{\tau}_{i,M,k}\\
&\text{z coordinate : } f^{\tau}_{i,j,1}=f^{\tau}_{i,j,2} \text{ or } f^{\tau}_{i,j,N+1}=f^{\tau}_{i,j,N} \text{ or } f^{\tau}_{i,j,1}=f^{\tau}_{i,j,2} \text{ and } f^{\tau}_{i,j,N+1}=f^{\tau}_{i,j,N}
\end{aligned} \quad (9)$$

Formation of Matrix

For example, $\left[\frac{\partial^2}{\partial \mathbf{x}^2}\right]$ could be represented by (10) as a matrix form.

$$\left[\frac{\partial^2}{\partial \mathbf{x}^2}\right]=\begin{bmatrix} 0 & 0 & 0 & \cdots & 0 & 0 & 0 \\ \hline \frac{1}{(\Delta x_2)^0(\Delta x_2)^-} & \frac{-2}{(\Delta x_2)^+(\Delta x_2)^-} & \frac{1}{(\Delta x_2)^+(\Delta x_2)^0} & 0 & \cdots & 0 & 0 \\ 0 & \frac{1}{(\Delta x_3)^0(\Delta x_3)^-} & \frac{-2}{(\Delta x_3)^+(\Delta x_3)^-} & \frac{1}{(\Delta x_3)^+(\Delta x_3)^0} & 0 & \cdots & 0 \\ \vdots & \ddots & \ddots & \ddots & \ddots & \ddots & \vdots \\ 0 & \cdots & 0 & \frac{1}{(\Delta x_{L-1})^0(\Delta x_{L-1})^-} & \frac{-2}{(\Delta x_{L-1})^+(\Delta x_{L-1})^-} & \frac{1}{(\Delta x_{L-1})^+(\Delta x_{L-1})^0} & 0 \\ 0 & 0 & \cdots & 0 & \frac{1}{(\Delta x_L)^0(\Delta x_L)^-} & \frac{-2}{(\Delta x_L)^+(\Delta x_L)^-} & \frac{1}{(\Delta x_L)^+(\Delta x_L)^0} \\ \hline 0 & 0 & 0 & \cdots & 0 & 0 & 0 \end{bmatrix} \quad (10)$$

$$=\begin{bmatrix} \mathbf{0} \\ \hline \left(\frac{\partial^2}{\partial \mathbf{x}^2}\right)_{2\sim L} \\ \hline \mathbf{0} \end{bmatrix}$$

The matrix (10) is a square matrix composed of $(L+1)\times(L+1)$. To obtain the elements of the first row, the history at $(\Delta x_1)^-$ is required as well as x_0. However, x_0 is not yet defined. Thus, the elements of the first row are all zero. Since x_{L+2} is not defined for $(\Delta x_{L+1})^+$, the elements of the $(L+1)^{th}$ column of the matrix are all zero. As a result, the matrix $\left[\frac{\partial^2}{\partial \mathbf{x}^2}\right]$ is composed of second order derivatives from the second and to L^{th} rows. In addition, the first and $(L + 1)$ rows are formed by boundary conditions.

Formation of Matrix with Boundary Conditions

When a matrix **A** has Neumann boundary condition at node 1, Dirichlet boundary condition at node $L + 1$, and the second order derivatives of the matrix **A** is the same as a matrix **B**, (11) can be written.

$$\frac{\partial^2 \mathbf{A}}{\partial x^2}=\mathbf{B} \quad (11)$$

As a matrix form of (11) can be (12)

$$\mathbf{M}\cdot\mathbf{A}=\mathbf{B} \quad (12)$$

where **M** has a following form.

$$M=\underbrace{\begin{bmatrix} \mathbf{0} \\ \hline \left(\frac{\partial^2}{\partial \mathbf{x}^2}\right)_{2\sim L} \\ \hline \mathbf{0} \end{bmatrix}}_{\text{matrix of second order derivaties for 2\textasciitilde L rows}}+\underbrace{\begin{bmatrix} 1 \quad -1 & \\ \hline \mathbf{0} \\ \hline & 1 \end{bmatrix}}_{\text{matrix of boundary conditions}}=\begin{bmatrix} 1 \quad -1 & \\ \hline \left(\frac{\partial^2}{\partial \mathbf{x}^2}\right)_{2\sim L} \\ \hline & 1 \end{bmatrix}$$

Therefore, (12) can be represented by (13)

$$\begin{bmatrix} 1 \quad -1 & \\ \hline \left(\frac{\partial^2}{\partial \mathbf{x}^2}\right)_{2\sim L} \\ \hline & 1 \end{bmatrix}\begin{Bmatrix} a_1 \\ a_2 \\ \vdots \\ a_L \\ a_{L+1} \end{Bmatrix}=\begin{Bmatrix} 0 \\ b_2 \\ \vdots \\ b_L \\ 0 \end{Bmatrix} \quad (13)$$

Verification

Verification of theoretical approach was accomplished by comparing with the reference method [Bazant et al. (2004)]. As shown in Fig. 1, an external electrical potential is applied to the isolated ironic fluid.

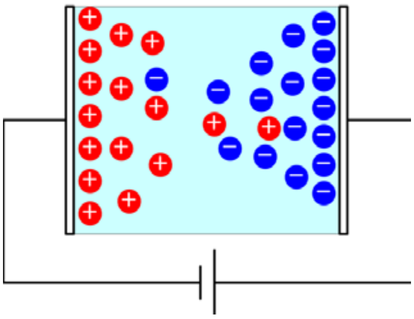

Figure 1. Electrolyte system affected by external electric field which induces the electric potential distribution of $\phi(y)$ with surface potential $\phi_L = -1.0$ V and $\phi_R = +1.0$ V

Analytical Method

The governing equation for the charge density can be represented by (14).

$$\frac{1}{D}\frac{\partial \rho_f}{\partial t} = \nabla^2 \rho_f - \kappa^2 \rho_f + \kappa^2 \varepsilon_f \nabla^2 \phi \qquad \nabla^2 \psi = -\rho_f / \varepsilon_f \tag{14}$$

ϕ is the external electrical potential generated by external electric field. For the external electrical potential, $\nabla^2 \phi = 0$. Thus, (14) is reduced to Debye-Falkenhagen equation (15).

$$\frac{1}{D}\frac{\partial \rho_f}{\partial t} = \nabla^2 \rho_f - \kappa^2 \rho_f \tag{15}$$

Based on (15), distributions of the electric charge density, ρ_f, change distributions and magnitudes of internal electric potential, ψ.

If ρ_f is a function of the only x-coordinate,

$$\frac{1}{D}\frac{\partial \rho_f}{\partial t} = \frac{\partial^2 \rho_f}{\partial x^2} - \kappa^2 \rho_f \tag{16}$$

where Φ is the total potential that is a summation of the external and internal potentials.

As assumed to be two plates, the one-dimensional boundary condition is represented by (17).

$$\frac{\partial \rho_f}{\partial x} = -\kappa^2 \varepsilon_f \left.\frac{\partial \Phi}{\partial x}\right|_{at\ x=\pm h} = -\kappa^2 \varepsilon_f \left.\left(\frac{\partial \psi}{\partial x} + \frac{\partial \phi}{\partial x}\right)\right|_{at\ x=\pm h} \tag{17}$$

A general solution of (17) in the Laplace domain (s-domain) can be obtained by (18) [Bazant et al. (2004)].

$$\hat{\rho}_f(x,s) = A(s)\sinh(kx) \tag{18}$$

where $A(s) = \dfrac{-k^2 \varepsilon_f V s^{-1} \operatorname{sech}(kh)}{\tanh(kh) + \lambda_s k + \dfrac{ksh}{\kappa^2 D}\left(1 + \dfrac{\lambda_s}{h}\right)}$, $\quad k^2 = \dfrac{s}{D} + \kappa^2$.

Table 1. Symbols

Symbols	Definitions
ρ_f	charge density
ψ	internal potential due to charge density distribution
ϕ	external potential due to external electric field
D	diffusion coefficient
κ	inverse of Debye length
ε_f	dielectric permittivity
h	half channel height
λ_s	effective thickness for the compact part of the double layer
V	external potential imposed by the external circuit

Numerical Method

The governing equation for the charge density can be discretized by (19).

$$\frac{1}{D}\frac{\rho_f^{t+1}-\rho_f^{t}}{\Delta t}-\nabla^2\rho_f^{t+1}+\kappa^2\rho_f^{t+1}=\kappa^2\varepsilon_f\nabla^2\phi^{t+1}$$
$$\left(\frac{1}{D\Delta t}-\nabla^2+\kappa^2\right)\rho_f^{t+1}=\frac{1}{D\Delta t}\rho_f^{t}+\kappa^2\varepsilon_f\nabla^2\phi^{t+1} \tag{19}$$

When ρ_f is a function of the only x-coordinate,

$$\frac{1}{D}\frac{\rho_f^{t+1}-\rho_f^{t}}{\Delta t}-\left[\frac{\partial^2}{\partial \mathbf{x}^2}\right]\rho_f^{t+1}+\kappa^2\rho_f^{t+1}=\kappa^2\varepsilon_f\left[\frac{\partial^2}{\partial \mathbf{x}^2}\right]\phi^{t+1} \tag{20}$$

Boundary condition

The boundary conditions can be represented by (21).

$$\rho_{f\,1}-\rho_{f\,2}=-\kappa^2\varepsilon_f\left[(\psi_1-\psi_2)+(\phi_1-\phi_2)\right]$$
$$\rho_{f\,L}-\rho_{f\,L+1}=-\kappa^2\varepsilon_f\left[(\psi_L-\psi_{L+1})+(\phi_L-\phi_{L+1})\right] \tag{21}$$

At the interface, the internal potential should be 0 to satisfy $\psi_{L+1}=\psi_1=0$. Then, (21) turns out to be (22).

$$\rho_{f\,1}-\rho_{f\,2}=-\kappa^2\varepsilon_f\left[\psi_2+(\phi_1-\phi_2)\right]$$
$$\rho_{f\,L}-\rho_{f\,L+1}=-\kappa^2\varepsilon_f\left[\psi_L+(\phi_L-\phi_{L+1})\right] \tag{22}$$

The governing equation (20) can be described by (23).

$$\left(\frac{1}{D\Delta t}\begin{bmatrix} & \mathbf{0} & \\ \mathbf{0} & \mathbf{I} & \mathbf{0} \\ & \mathbf{0} & \end{bmatrix} + \begin{bmatrix} \mathbf{0} \\ \left(\frac{\partial^2}{\partial \mathbf{x}^2}\right)_{2\sim L} \\ \mathbf{0} \end{bmatrix} + \kappa^2 \begin{bmatrix} & \mathbf{0} & \\ \mathbf{0} & \mathbf{I} & \mathbf{0} \\ & \mathbf{0} & \end{bmatrix}\right)\begin{Bmatrix} \rho_{f_1} \\ \rho_{f_2} \\ \vdots \\ \rho_{f_L} \\ \rho_{f_{L+1}} \end{Bmatrix}_{j,k}^{t+1} = \tag{23}$$

$$\frac{1}{D\Delta t}\begin{bmatrix} & \mathbf{0} & \\ \mathbf{0} & \mathbf{I} & \mathbf{0} \\ & \mathbf{0} & \end{bmatrix}\begin{Bmatrix} \rho_{f_1} \\ \rho_{f_2} \\ \vdots \\ \rho_{f_L} \\ \rho_{f_{L+1}} \end{Bmatrix}_{j,k}^{t} + \kappa^2 \varepsilon_f \begin{bmatrix} \mathbf{0} \\ \left(\frac{\partial^2}{\partial \mathbf{x}^2}\right)_{2\sim L} \\ \mathbf{0} \end{bmatrix}\begin{Bmatrix} \phi_1 \\ \phi_2 \\ \vdots \\ \phi_L \\ \phi_{L+1} \end{Bmatrix}_{j,k}^{t+1}$$

The boundary conditions (22) can be represented by (24).

$$\begin{bmatrix} 1 & -1 & & \\ & \mathbf{0} & & \\ & & 1 & -1 \end{bmatrix}\begin{Bmatrix} \rho_{f_1} \\ \rho_{f_2} \\ \vdots \\ \rho_{f_L} \\ \rho_{f_{L+1}} \end{Bmatrix}_{j,k}^{t+1} = \kappa^2 \varepsilon_f \begin{bmatrix} 0 & -1 & & \\ & \mathbf{0} & & \\ & & 1 & -1 \end{bmatrix}\begin{Bmatrix} \psi_1 \\ \psi_2 \\ \vdots \\ \psi_L \\ \psi_{L+1} \end{Bmatrix}_{j,k}^{t+1} + \kappa^2 \varepsilon_f \begin{bmatrix} 1 & -1 & & \\ & \mathbf{0} & & \\ & & 1 & -1 \end{bmatrix}\begin{Bmatrix} \phi_1 \\ \phi_2 \\ \vdots \\ \phi_L \\ \phi_{L+1} \end{Bmatrix}_{j,k}^{t+1} \tag{24}$$

After combining the boundary conditions to the governing equation, the final form can be obtained as (25).

$$\therefore \begin{Bmatrix} \rho_{f_1} \\ \rho_{f_2} \\ \vdots \\ \rho_{f_L} \\ \rho_{f_{L+1}} \end{Bmatrix}_{j,k}^{t+1} = \left\langle \frac{1}{D\Delta t}\begin{bmatrix} & \mathbf{0} & \\ \mathbf{0} & \mathbf{I} & \mathbf{0} \\ & \mathbf{0} & \end{bmatrix} + \begin{bmatrix} \mathbf{0} \\ \left(\frac{\partial^2}{\partial \mathbf{x}^2}\right)_{2\sim L} \\ \mathbf{0} \end{bmatrix} + \kappa^2 \begin{bmatrix} & \mathbf{0} & \\ \mathbf{0} & \mathbf{I} & \mathbf{0} \\ & \mathbf{0} & \end{bmatrix} + \begin{bmatrix} 1 & -1 & & \\ & \mathbf{0} & & \\ & & 1 & -1 \end{bmatrix} \right\rangle^{-1}$$
$$\cdot \left\langle \frac{1}{D\Delta t}\begin{bmatrix} & \mathbf{0} & \\ \mathbf{0} & \mathbf{I} & \mathbf{0} \\ & \mathbf{0} & \end{bmatrix}\begin{Bmatrix} \rho_{f_1} \\ \rho_{f_2} \\ \vdots \\ \rho_{f_L} \\ \rho_{f_{L+1}} \end{Bmatrix}_{j,k}^{t} + \kappa^2 \varepsilon_f \left(\begin{bmatrix} \mathbf{0} \\ \left(\frac{\partial^2}{\partial \mathbf{x}^2}\right)_{2\sim L} \\ \mathbf{0} \end{bmatrix} + \begin{bmatrix} 1 & -1 & & \\ & \mathbf{0} & & \\ & & 1 & -1 \end{bmatrix}\right)\begin{Bmatrix} \phi_1 \\ \phi_2 \\ \vdots \\ \phi_L \\ \phi_{L+1} \end{Bmatrix}_{j,k}^{t+1} + \kappa^2 \varepsilon_f \begin{bmatrix} 0 & -1 & & \\ & \mathbf{0} & & \\ & & 1 & -1 \end{bmatrix}\begin{Bmatrix} \psi_1 \\ \psi_2 \\ \vdots \\ \psi_L \\ \psi_{L+1} \end{Bmatrix}_{j,k}^{t+1} \right\rangle \tag{25}$$

Table 2. Properties used in this study

Symbols	Values
D	1.0×10^{-17} $[m]$
κ	1.29×10^{9} $[1/m]$
ε_f	6.94×10^{-10} $[C/Vm]$
h	1.0×10^{-8} $[m]$
λ_s	5.0×10^{-10} $[m]$
V	$1.0\,[V]$

Utilizing the data in Tab. 2, transient behaviors of the charge density in the space are calculated and compared in Fig. 2 from the closed form solution and the numerical method proposed in this study. In general, the results from the analytic and numerical methods are in agreement for each time as shown in Tab. 3. In transient analyses, the behavior from the numerical method has a time-delay of 0.01 sec than that from the analysis. However, two behaviors from the numerical method and analysis in steady state are almost identical in time and space.

Table 3. Defined variances* for comparisons of numerical solutions on analytic results

Time [sec]	Values [dimensionless]
0.1	4.5042×10^{-2}
0.2	4.1764×10^{-2}
0.5	3.4787×10^{-2}
1.0	2.5344×10^{-2}
Steady State	2.3630×10^{-3}

*Defined variance: $s^2 = \frac{1}{n-1}\sum_{j=1}^{n}\left(\frac{x_{numerical\ j} - x_{analytic\ j}}{x_{analytic\ j}}\right)^2$

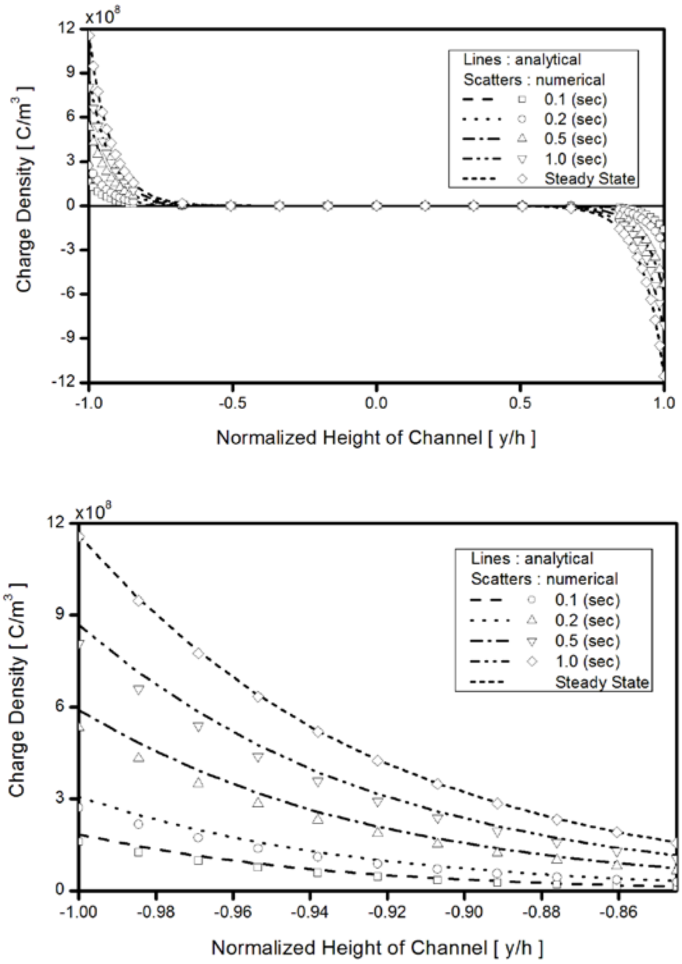

Figure 2. Comparisons of the analytic solutions on the numerical results (upper : total charge distribution and lower : magnified left side)

Conclusion

In electrokinetics, accurate prediction of the temporal and spatial charge density distributions near the ironic fluid and piezoelectric solid interface become important from the multi-physical point of view. Since the interested region for the changes of charge density distribution is the order of 10 Angstrom just near the interface, a very fine FD grid is required. When a constant fine space increment is applied for electrokinetic problems to obtain an accurate solution using FDM, the calculation process is inefficient.

In this study, FDM using the nonhomogeneous space increment is formulated and applied to an electrokinetic problem. A very fine FD grid is used for the interested diffuse layer just near the interface. At the same time, coarse FD grids are applied to the other ironic fluid path that is the order of several nanometers. In addition, a governing equation matrix is combined with a boundary condition matrix to construct an integrated equation matrix. As a result, PDE problems having mixed boundary conditions could be easily formulated and numerically solved by the proposed FDM using the simple matrix method.

In addition, the formulated FDM using the simple matrix method becomes a fully implicit form for space. Therefore, effects of amount of space increment on solution procedures could be minimized. The proposed method could be useful for obtaining transient solutions in electrokinetic problems particularly for bone remodeling, which electrical potentials are being changed temporally and spatially by the piezoelectricity of bone matrix.

Acknowledgment

This work was sponsored by the National Research Foundation of Korea (NRF) grants (No. 2012R1A2A2A01016829 and No. 2010-0001151) funded by the Korean Ministry of Science, ICT and Future Planning.

References

Ahn, A. C., and Grodzinsky, A. J. (2009) Relevance of collagen piezoelectricity to "Wolff's Law": A critical review, *Medical Engineering and Physics* **31**, 733-74.

Bazant, M. J., Thornton, K., and Ajdari, A. (2004) Diffuse-charge dynamics in electrochemical systems, *Physical Review E* **70**, 021506–1–54.

Bassett, C. A. (1968), Biologic significance of piezoelectricity, *Calcified Tissue Research* **1**, 252-272.

Pienkowski, D., and Pollack, S. R. (1983) The origin of stress-generated potentials in fluid-saturated bone, *Journal of Orthpaedic Research* **1**, 30-41.

Zhang, D., Cowin, S. C., Weinbaum, S. (1997) Electrical signal transmission and gap junction regulation in a bone cell network: a cable model for an osteon, *Annals of Biomedical Engineering* **25**, 357-374.